Int. Journal of Refractory Metals and Hard Materials 41 (2013) 437–441

Contents lists available at ScienceDirect

Int. Journal of Refractory Metals and Hard Materials

journal homepage: www.elsevier.com/locate/IJRMHM

Properties of porous alumina ceramics prepared by technique combining cold-drying and sintering

Xiangming Li, Pute Wu *, Delan Zhu

Institute of Water Saving Agriculture in Arid Areas of China, Northwest A&F University, Yangling, Shaanxi 712100, PR China

ARTICLE INFO

Article history:
Received 16 April 2013
Accepted 26 May 2013

Keywords:
Porous
Alumina
Microstructure
Porosity
Flexural strength

ABSTRACT

For preparing porous alumina ceramics with desired shapes easily, a simple and low-cost technique combining cold-drying and sintering was explored. The optimal temperature for preparing the porous alumina ceramics is 1350 °C. The contents of $CaCO_3$–SiO_2 and dextrin in the green body have great effects on the properties of porous alumina ceramics. Due to a uniform microstructure and small pore size, the porous alumina ceramics prepared from the green body with 8 wt.% $CaCO_3$–SiO_2 show higher flexural strength and porosity. As the dextrin in the green body increases from 5 to 25 wt.%, the flexural strength decreases from 107 to 45 MPa with the porosity increasing from 36 to 54%.

1. Introduction

Recently, increasing attention has been attracted by porous ceramics because of their expanding technological applications in a wide range of fields [1–9], especially for separation materials [3,4], catalyst supports [5,6], and implantable bioceramics [7,8]. Due to their low density, good thermal conductivity, chemical durability and refractoriness, porous alumina ceramics have been frequently used at high temperature environments and under severe chemical conditions [4–6,8,9]. Sintering is a conventional preparation method for preparing porous alumina ceramics, and cold-pressing is the most common technique to prepare the green body. However, cold-pressing is suitable only for preparing ceramics with simple shapes. In order to make porous alumina ceramics possess a desired shape, grinding is a necessary remachining technique which involves high expense and is difficult to operate.

Various advanced routes have been developed to prepare porous alumina ceramics, such as gelcasting [9–12], freezing [13–15], ice templating [16], and direct forming [17]. In the present paper, for preparing porous alumina ceramics with desired shapes easily, a simple and low-cost technique combining cold-drying and sintering was explored. The effects of the preparation parameters on the microstructure, porosity and flexural strength of the porous alumina ceramics are studied in detail, and the optimal preparation parameters are discussed.

2. Experimental

2.1. Preparation process

Alumina powder (α ratio > 99.9 wt.%, mean grain size of 3 μm) was mixed with $CaCO_3$ (analytically pure, mean grain size of 40–50 nm), dextrin and silica sol (SiO_2 = 30 ± 1 wt.%, NaO_2 ≤ 0.3 wt.%, SiO_2 mean grain size of 8–15 nm), and then the mixture was placed in distilled water and ball milled (rotation speed of 180 r/min, revolution speed of 200 r/min) for 10 h into a slurry. The slurry was poured into rectangular Al_2O_3 moulds with cavity dimensions of 5 mm × 10 mm × 50 mm, and then put together with the Al_2O_3 moulds into a closed container. At 3–5 °C, the slurry in the Al_2O_3 moulds turned into green bodies by keeping the pressure in the container lower than 2 kPa for 24 h. Finally, the green bodies were taken out and pre-oxidized in air at 800 °C for 5 h, and then sintered into porous alumina ceramics at 1200, 1250, 1300, 1350 and 1400 °C respectively for 2 h.

In the above preparation process, the dextrin in the slurry plays two roles, one is the viscosity regulator of the slurry, and the other is acting as the pore-forming agent of the ceramics during pre-oxidation process. By changing the proportions of the different components and distilled water in the raw mixture, the dynamic viscosity of the slurry is controlled at 0.8–0.9 Pa · s which is suitable for slip casting [18]. In the green body, the mole ratio of $CaCO_3$ and SiO_2 was 1:1, the content of $CaCO_3$–SiO_2 was defined respectively at 4, 8,

* Corresponding author. Tel.: +86 29 87092860; fax: +86 29 87012210.
E-mail address: gjzwpt@vip.sina.com (P. Wu).

0263-4368/$ – see front matter © 2013 Elsevier Ltd. All rights reserved.
http://dx.doi.org/10.1016/j.ijrmhm.2013.05.020

12 and 16 wt.%, and the content of dextrin was controlled respectively at 5, 10, 15, 20 and 25 wt.%.

2.2. Characterization and tests

The microstructure was observed by using scanning electron microscopy (JSM-6360LV, Electronics Co., Ltd., Japan). The porosity and the density were measured by using the Archimedes method. The pore size distributions were measured by a mercury porosimeter (Poremaster 33, Quantachrome Instruments Co., Boynton Beach, FL, USA). Phase analysis was conducted by X-ray diffraction (XRD) using a powder test method, via a computer-controlled diffractometer (X'Pert Pro, Philips, Netherlands). Using a CMT4204 instrument (Jiehu Instrument Co., Ltd. Shanghai, China), the flexural strength of the specimens with a dimension of 3 mm × 4 mm × 40 mm were evaluated via the three-point bending test with a support distance of 30 mm and at a loading speed of 0.05 mm/min. Before flexural strength testing, the specimens were polished with a 0.5 μm diamond paste as a final polishing step, and then ultrasonically cleaned in acetone and air-dried.

For the convenience of the following discussion, the porous alumina ceramics prepared from the green body with different contents of $CaCO_3$–SiO_2 and dextrin are named as Al_2O_3–*m*–*n* (*m* stands for the content of $CaCO_3$–SiO_2, *n* stands for the content of dextrin).

3. Results and discussion

Porosity and flexural strength are two important properties of porous ceramics, which are strongly influenced by the sintering temperature [19]. Generally, after sintering at high temperature, the porous ceramics obtain high flexural strength because of good sintering but get relatively low porosity due to large shrinkage [20]. If the sintering temperature is low, the porous ceramics show bad flexural strength due to inadequate sintering. For preparing porous alumina ceramics with high flexural strength and high porosity at the same time, the first thing is to determine the optimal sintering temperature.

Fig. 1 shows the XRD patterns of the porous alumina ceramic sintering at different temperatures from the green body with 16 wt.% $CaCO_3$–SiO_2. In spite of the peaks of the primary phase of α-Al_2O_3, the other phases change gradually with the sintering temperature rising. When the sintering temperature is 1200 °C, the peaks of CaO and SiO_2 can be seen clearly in the XRD pattern. As the temperature rises, the peaks of CaO and SiO_2 disappear slowly, and the peaks of $Ca_2Al_2SiO_7$ appear gradually. $Ca_2Al_2SiO_7$ is a solid solution phase existing among alumina grains which decides the sintering of the porous alumina ceramics [21,22]. Except for the peaks of alumina, there are only peaks of $Ca_2Al_2SiO_7$ in the XRD pattern when the temperature is higher than 1350 °C, which indicates a complete

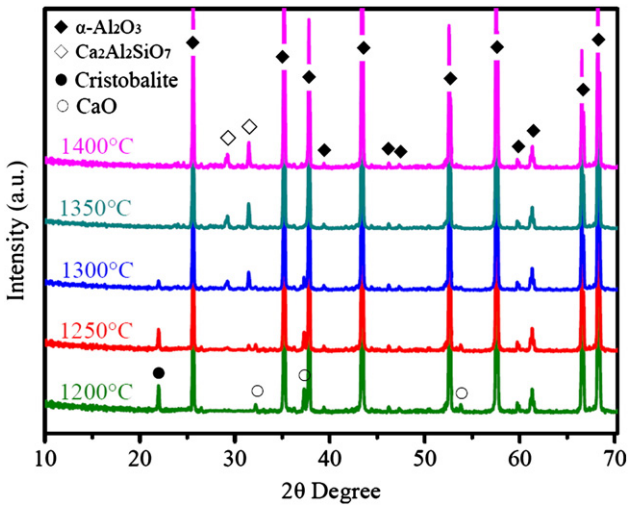

Fig. 1. XRD patterns of the porous alumina ceramic sintering at different temperatures from the green body with 16 wt.% $CaCO_3$–SiO_2.

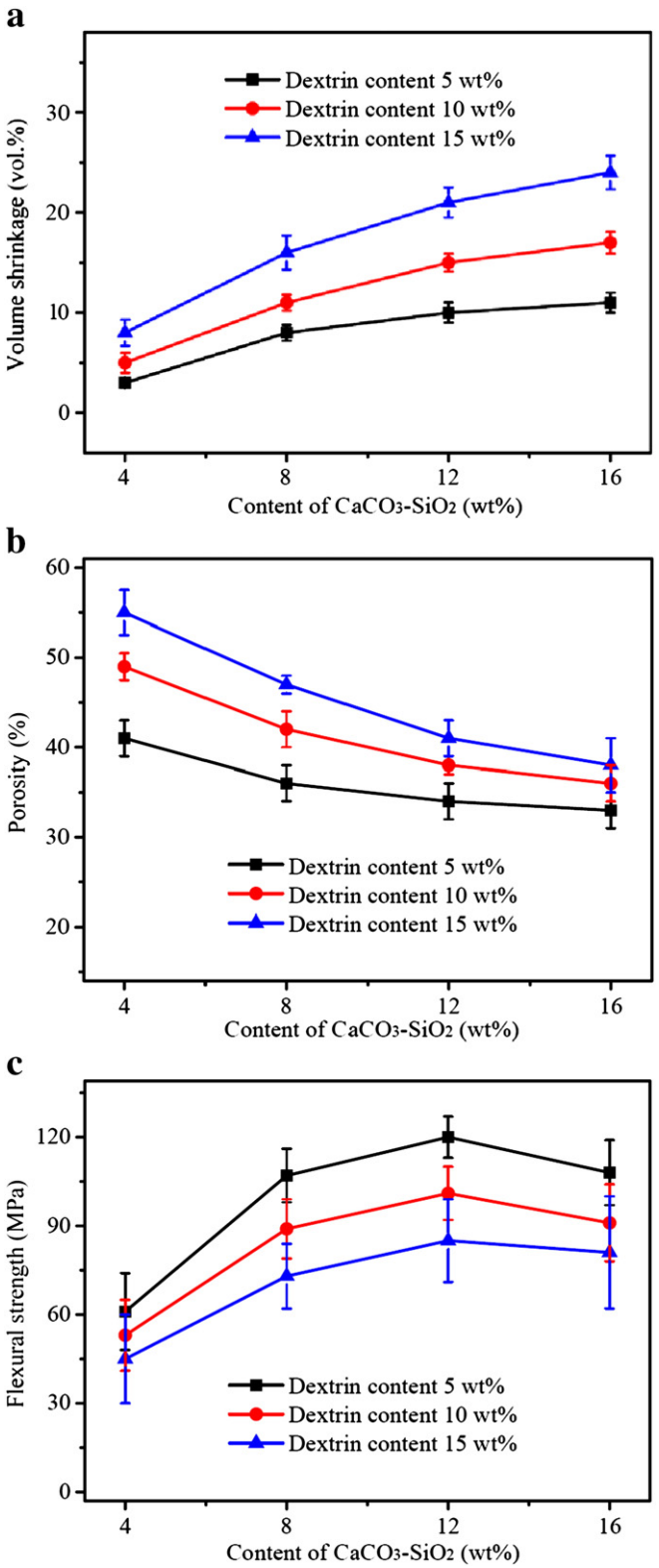

Fig. 2. (a) Volume shrinkage, (b) porosity and (c) flexural strength of porous alumina ceramics as functions of $CaCO_3$–SiO_2 content in the green body.

reaction of CaO and SiO_2. Accordingly, 1350 °C is the optimal sintering temperature for preparing porous alumina ceramics.

Fig. 2 shows the volume shrinkage, porosity and flexural strength of porous alumina ceramics as functions of the $CaCO_3$–SiO_2 content in the green body. During the sintering process, the CaO and SiO_2 react with alumina grains and form $Ca_2Al_2SiO_7$ which is the liquid phase at elevated temperatures [21,22]. With the help of the reaction-derived liquid $Ca_2Al_2SiO_7$ at elevated temperatures, the alumina grains are dragged close to each other. The more the $CaCO_3$–SiO_2 content in the green body, the more $Ca_2Al_2SiO_7$ is produced, and the closer the alumina grains are dragged together, so the volume shrinkage of porous alumina ceramics increases with the content of $CaCO_3$–SiO_2 in the green body increasing, as shown in Fig. 2(a). Due to the increase of volume shrinkage, the porous alumina ceramics decrease in porosity with the content of $CaCO_3$–SiO_2 in the green body increasing, as shown in Fig. 2(b). Take Al_2O_3–n10 as an example, as the content of $CaCO_3$–SiO_2 in the green body increases from 4 to 16 wt.%, Al_2O_3–n10 increases in volume shrinkage from 5 to 17% and decreases in porosity from 49 to 36%.

In the green body, the dextrin exists among the alumina grains, and the distance between the alumina grains gets larger with the dextrin content in the green body increasing, so the porosity of porous alumina ceramics increases with the dextrin content in the green body increasing, as shown in Fig. 2(b). On the other hand, the distance between the alumina grains decreases because of the dragging effect of the reaction-derived liquid $Ca_2Al_2SiO_7$ during the sintering process, and the dragging effect becomes obvious with the distance between the alumina grains increasing. Therefore, the volume shrinkage of porous alumina ceramics increases with the dextrin content in the green body increasing, as shown in Fig. 2(a).

At elevated temperatures, the liquid $Ca_2Al_2SiO_7$ on the surface of the alumina grains promotes the sintering of porous alumina ceramics, so the flexural strength of porous alumina ceramics increases with the content of $CaCO_3$–SiO_2 in the green body increasing from 4 to 12 wt.%, as shown in Fig. 2(c). However, too much $CaCO_3$–SiO_2 in the green body produces excessive $Ca_2Al_2SiO_7$, the flexural strength of which is lower than that of the alumina grains, and excessive $Ca_2Al_2SiO_7$ also causes exaggerated growth of alumina grains, so the flexural strength of porous alumina ceramics decreases on the contrary as the $CaCO_3$–SiO_2 content in the green body increases from 12 to 16 wt.%. Take Al_2O_3–n10 as an example, the flexural strength increases from 53 to 101 MPa with the content of $CaCO_3$–SiO_2 increasing from 4 to 12 wt.%, and then decreases to 91 MPa as the content of $CaCO_3$–SiO_2 further increases to 16 wt.%. In addition, because of the increase of porosity, the porous alumina ceramics decrease in flexural strength with the dextrin content in the green body increasing. Take Al_2O_3–m12 as an example, the flexural strength of porous alumina ceramics decreases from 120 to 85 MPa with the dextrin content in the green body increasing from 5 to 15 wt.%.

Fig. 3 shows the XRD patterns of the porous alumina ceramic sintering at 1350 °C from the green body with a different $CaCO_3$–SiO_2 content. As can be seen, the peaks of $Ca_2Al_2SiO_7$ increase with the $CaCO_3$–SiO_2 content in the green body increasing from 4 to 16 wt.%, and the peaks of $Ca_2Al_2SiO_7$ are apparent when the $CaCO_3$–SiO_2 content in the green body is higher than 8 wt.%. According to the results shown in Figs. 2 and 3, the suitable content of $CaCO_3$–SiO_2 in the green body is in the range of 8–12 wt.%.

Fig. 4 shows the porosities of Al_2O_3–m8 and Al_2O_3–m12 fabricated from the green bodies with a different dextrin content. As the dextrin content in the green body increases from 5 to 25 wt.%, the porosity of Al_2O_3–m8 and Al_2O_3–m12 increases respectively from 36 to 54% and 34 to 46%. As known from the results shown in Fig. 4, the porous alumina ceramics prepared from the green bodies with 12 wt.% $CaCO_3$–SiO_2 show higher porosity than that of the ones prepared from the green bodies with 8 wt.% $CaCO_3$–SiO_2. Therefore, the porosity of porous alumina ceramics may be increased theoretically by decreasing the $CaCO_3$–SiO_2 content or increasing the dextrin content in the green body. However, these two approaches have totally different effects on the microstructure and pore size of porous alumina ceramics.

Take the porous alumina ceramics with the same porosity as example, Fig. 5 shows the micrographs of Al_2O_3–m8–n10 and Al_2O_3–m12–n15. As can be seen, the pores in Al_2O_3–m8–n10 and Al_2O_3–m12–n15 exist among the alumina grains and distribute evenly throughout the whole sample, but the microstructures of Al_2O_3–m8–n10 and Al_2O_3–m12–n15 are much different from each other. Excessive $Ca_2Al_2SiO_7$ causes exaggerated growth of alumina grains, so the alumina grains in Al_2O_3–m12–n15 are bigger than those in Al_2O_3–m8–n10. For this reason, the pores among the alumina grains in Al_2O_3–m12–n15 are much bigger than those in Al_2O_3–m8–n10. As a whole, the microstructure of Al_2O_3–m8–n10 is more uniform than that of Al_2O_3–m12–n15.

Fig. 6 compares the pore size distribution patterns of Al_2O_3–m8–n10 and Al_2O_3–m12–n15. The pore size distributions were measured by a mercury porosimeter. During the measuring process, the pressure for the mercury intruding into the porous alumina ceramics increases with the pore size of the porous alumina ceramics

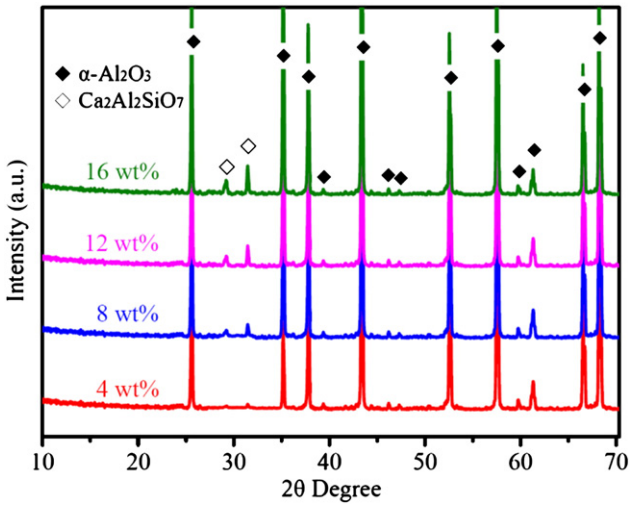

Fig. 3. XRD patterns of the porous alumina ceramic sintering at 1350 °C from the green body with different $CaCO_3$–SiO_2 content.

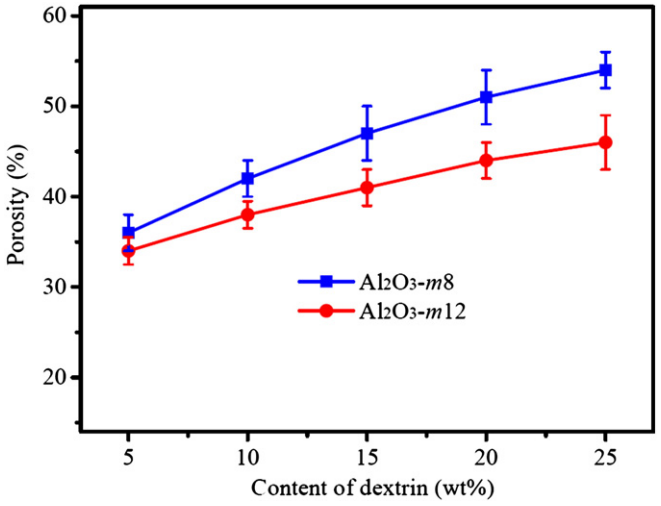

Fig. 4. Porosities of Al_2O_3–m8 and Al_2O_3–m12 fabricated from the green bodies with different dextrin content.

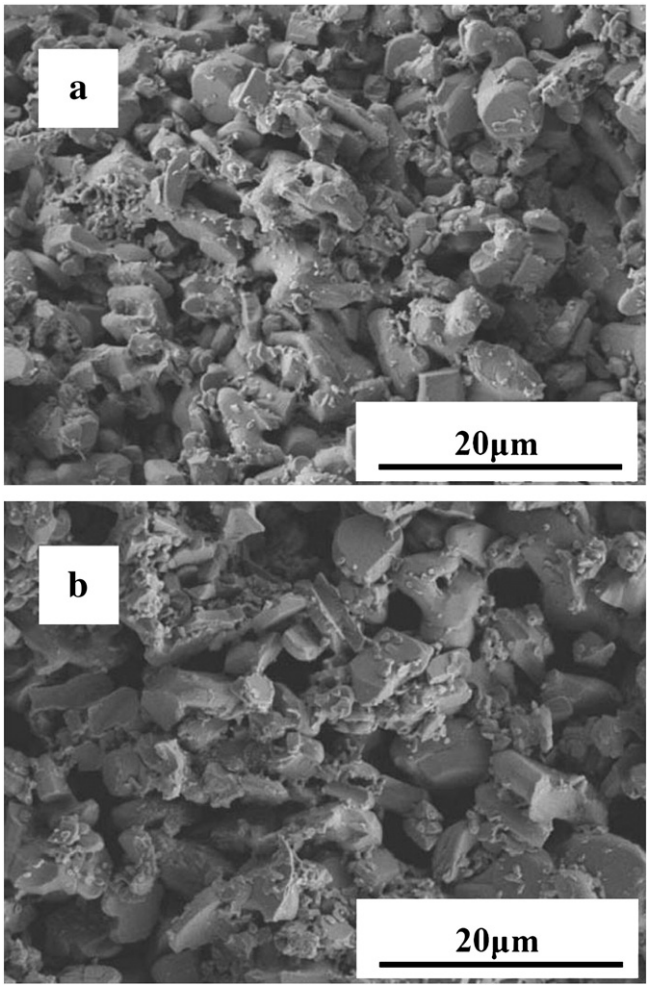

Fig. 5. Micrographs of (a) Al_2O_3–*m*8–*n*10 and (b) Al_2O_3–*m*12–*n*15.

decreasing, so the pore size distribution is just the variation of the amount of mercury intrusion. As shown in Fig. 6, the pore size for mercury intruding into Al_2O_3–*m*12–*n*15 is obviously larger than that of mercury intruding into Al_2O_3–*m*8–*n*10, which means the pore size of Al_2O_3–*m*12–*n*15 is much larger than that of Al_2O_3–*m*8–*n*10. And, the pore size distribution pattern of Al_2O_3–*m*8–*n*10 is narrow and the pore size mainly concentrates upon 0.4–2 μm, while the

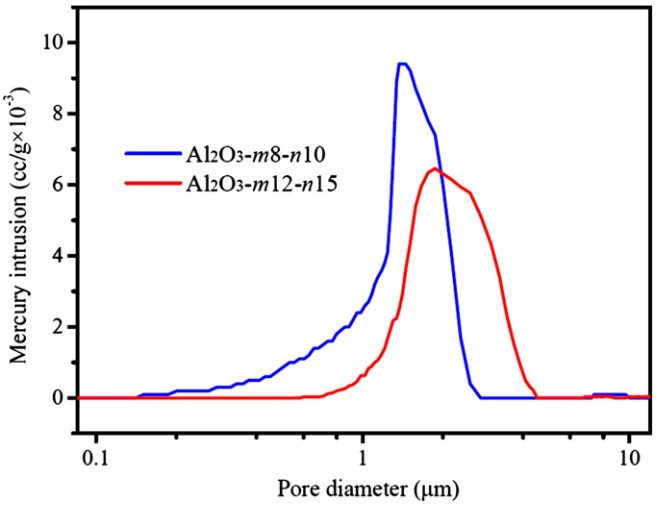

Fig. 6. Pore size distribution patterns of (a) Al_2O_3–*m*8–*n*10 and (b) Al_2O_3–*m*12–*n*15.

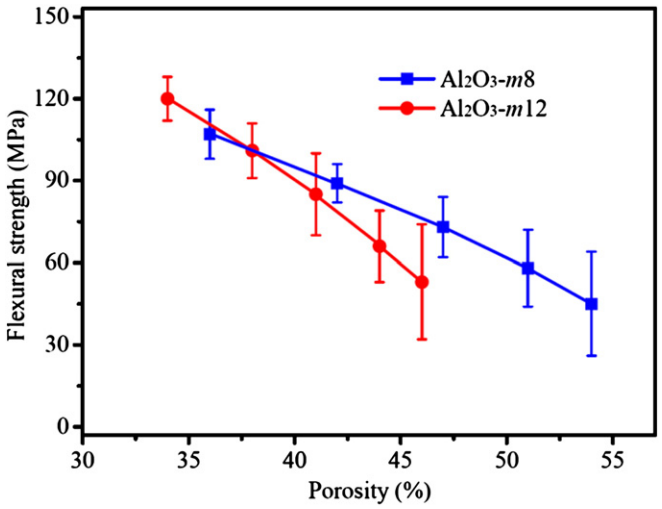

Fig. 7. Flexural strength of Al_2O_3–*m*8 and Al_2O_3–*m*12 as functions of porosity.

pore size distribution pattern of Al_2O_3–*m*12–*n*15 is relatively wide and the mean pore size is ranging from 1 to 4 μm.

Fig. 7 shows the flexural strength of Al_2O_3–*m*8 and Al_2O_3–*m*12 as functions of porosity. The flexural strength of these two porous alumina ceramics both decrease with the porosity increasing. The flexural strength of Al_2O_3–*m*8 decreases from 107 to 45 MPa with the porosity increasing from 36 to 54%, while the flexural strength of Al_2O_3–*m*12 decreases from 120 to 53 MPa with the porosity increasing from 34 to 46%. As known from Figs. 5 and 6, the porous alumina ceramics with the same porosity but prepared from the green body with different contents of $CaCO_3$–SiO_2 and dextrin show much different microstructures and pore size distributions. These differences influence greatly the flexural strength of the porous alumina ceramics. As shown in Fig. 7, although the porosity of Al_2O_3–*m*8 is higher than that of Al_2O_3–*m*12, Al_2O_3–*m*8 still possesses a higher flexural strength than that of Al_2O_3–*m*12 due to its uniform microstructure and small pore size.

4. Conclusions

Porous alumina ceramics with high porosity and good flexural structure were prepared by a simple and low-cost technique combining cold-drying and sintering. The sintering temperature and the contents of $CaCO_3$–SiO_2 and dextrin in the green body are three key factors influencing the properties of porous alumina ceramics. For preparing porous alumina ceramics with high porosity and flexural strength, the optimal sintering temperature is 1350 °C, and the optimal content of $CaCO_3$–SiO_2 in the green body is 8 wt.%. As the dextrin in the green body increases from 5 to 25 wt.%, the flexural strength of Al_2O_3–*m*8 decreases from 107 to 45 MPa with the porosity increasing from 36 to 54%. The porous alumina ceramics combine high porosity and good mechanical property, therefore proving themselves as promising structural/functional materials.

Acknowledgements

The authors gratefully acknowledge the financial support from the National Engineering Technology Research Center Reconstruction Project (2011FU125Z27-1) and the National Natural Science Foundation of China (No. 51209177). This work was also supported by the Basic Research Fund of Northwest A&F University (No. QN2012024) and the Dr. Scientific Start-up Funds of Northwest A&F University (2011BSJJ083).

References

[1] Abduljalil AS, Yu ZB, Jaworski AJ. Selection and experimental evaluation of low-cost porous materials for regenerator applications in thermoacoustic engines. Mater Des 2011;32:217–8.
[2] Li XM, Zhang LT, Yin XW. Fabrication and properties of porous Si_3N_4 ceramic with high porosity. J Mater Sci Technol 2012;28:1151–6.
[3] Kitaoka S, Matsushima Y, Chen C, Awaji H. Thermal cyclic fatigue behavior of porous ceramics for gas cleaning. J Am Ceram Soc 2004;87:906–13.
[4] Cheow PS, Ting EZC, Tan MQ, Toh CS. Transport and separation of proteins across platinum-coated nanoporous alumina membranes. Electrochim Acta 2008;53:4669–73.
[5] Naik B, Prasad VS, Ghosh NN. Preparation of Ag nanoparticle loaded mesoporous γ-alumina catalyst and its catalytic activity for reduction of 4-nitrophenol. Powder Technol 2012;232:1–6.
[6] Newnham J, Mantri K, Amin MH, Tardio J, Bhargava SK. Highly stable and active Ni-mesoporous alumina catalysts for dry reforming of methane. Int J Hydrogen Energy 2012;37:1454–64.
[7] Yoon BH, Koh YH, Park CS, Kim HE. Generation of large pore channels for bone tissue engineering using camphene-based freeze casting. J Am Ceram Soc 2007;90:1744–52.
[8] Yoon BH, Choi WY, Kim HE, Kim JH, Koh YH. Aligned porous alumina ceramics with high compressive strengths for bone tissue engineering. Scripta Mater 2008;58:537–40.
[9] Kitiwan M, Atong D. Effects of porous alumina support and plating time on electroless plating of palladium membrane. J Mater Sci Technol 2010;26:1148–52.
[10] Potoczek M. Gelcasting of alumina foams using agarose solutions. Ceram Int 2008;34:661–7.
[11] Takahashi M, Menchavez RL, Fuji M, Takegami H. Opportunities of porous ceramics fabricated by gelcasting in mitigating environmental issues. J Eur Ceram Soc 2009;29:823–8.
[12] Zou CR, Zhang CR, Li B, Wang SQ, Cao F. Microstructure and properties of porous silicon nitride ceramics prepared by gel-casting and gas pressure sintering. Mater Des 2013;44:114–8.
[13] Zhang YM, Hu LY, Han JC, Jiang ZH. Freeze casting of aqueous alumina slurries with glycerol for porous ceramics. Ceram Int 2010;36:617–21.
[14] Xia YF, Zeng YP, Jiang DL. Microstructure and mechanical properties of porous Si_3N_4 ceramics prepared by freeze-casting. Mater Des 2012;33:98–103.
[15] Zhang RB, Fang DN, Chen XM, Pei YM, Wang ZD, Wang YS. Microstructure and properties of highly porous Y_2SiO_5 ceramics produced by a new water-based freeze casting. Mater Des 2013;46:746–50.
[16] Zhang D, Meggs C, Button TWP. Porous Al_2O_3–ZrO_2 composites fabricated by an ice template method. Scripta Mater 2010;62:466–8.
[17] He X, Zhou XG, Su B. 3D interconnective porous alumina ceramics via direct protein foaming. Mater Lett 2009;63:830–2.
[18] Janney AM, Omatete OO. Method for molding ceramics powders using a water-based gel-casting process. US patent, No.5145908;1992.
[19] Li XM, Zhang LT, Yin XW. Microstructure and mechanical properties of three porous Si_3N_4 ceramics fabricated by different techniques. Mater Sci Eng A 2012;549:43–9.
[20] Wu SH, Wei XS, Wang XY, Yang HX, Gao SQ. Effect of Bi_2O_3 additive on the microstructure and dielectric properties of $BaTiO_3$-based ceramics sintered at lower temperature. J Mater Sci Technol 2010;26:472–6.
[21] Braulio MAL, Rigaud M, Buhr A, Parr C, Pandolfelli VC. Spinel-containing alumina-based refractory castables. Ceram Int 2011;37:1705–24.
[22] Souza TM, Braulio MAL, Luz AP, Bonadia P, Pandolfelli VC. Systemic analysis of MgO hydration effects on alumina–magnesia refractory castables. Ceram Int 2012;38:3969–76.